Typical somatomotor physiology of the hand is preserved in a patient with an amputated arm: An ECoG case study

Max van den Boom [a,b,*], Kai J. Miller [c], Nicholas M. Gregg [d], Gabriela Ojeda Valencia [a], Kendall H. Lee [c], Thomas J. Richner [c], Nick F. Ramsey [b], Greg A. Worrell [d], Dora Hermes [a,*]

[a] *Department of Physiology and Biomedical Engineering, Mayo Clinic Mayo Clinic, 200 First Street SW, Rochester, MN 55905, USA*
[b] *Department of Neurology & Neurosurgery, UMC Utrecht Brain Center, University Medical Center Utrecht, Heidelberglaan 100, 3584 CX Utrecht, The Netherlands*
[c] *Department of Neurosurgery, Mayo Clinic Mayo Clinic, 200 First Street SW, Rochester, MN 55905, USA*
[d] *Department of Neurology, Mayo Clinic Mayo Clinic, 200 First Street SW, Rochester, MN 55905, USA*

ABSTRACT

Electrophysiological signals in the human motor system may change in different ways after deafferentation, with some studies emphasizing reorganization while others propose retained physiology. Understanding whether motor electrophysiology is retained over longer periods of time can be invaluable for patients with paralysis (e.g. ALS or brainstem stroke) when signals from sensorimotor areas may be used for communication or control over neural prosthetic devices. In addition, a maintained electrophysiology can potentially benefit the treatment of phantom limb pains through prolonged use of these signals in a brain-machine interface (BCI).

Here, we were presented with the unique opportunity to investigate the physiology of the sensorimotor cortex in a patient with an amputated arm using electrocorticographic (ECoG) measurements. While implanted with an ECoG grid for clinical evaluation of electrical stimulation for phantom limb pain, the patient performed attempted finger movements with the contralateral (lost) hand and executed finger movements with the ipsilateral (healthy) hand.

The electrophysiology of the sensorimotor cortex contralateral to the amputated hand remained very similar to that of hand movement in healthy people, with a spatially focused increase of high-frequency band (65–175 Hz; HFB) power over the hand region and a distributed decrease in low-frequency band (15–28 Hz; LFB) power. The representation of the three different fingers (thumb, index and little) remained intact and HFB patterns could be decoded using support vector learning at single-trial classification accuracies of >90%, based on the first 1–3 s of the HFB response. These results indicate that hand representations are largely retained in the motor cortex. The intact physiological response of the amputated hand, the high distinguishability of the fingers and fast temporal peak are encouraging for neural prosthetic devices that target the sensorimotor cortex.

1. Introduction

Deafferentation from the loss of a limb affects the inputs and outputs to and from sensorimotor areas in the brain. However, it is not yet clear what happens to the physiology of these cortical regions when a limb is amputated. Using electrocorticography (ECoG) measurements in humans, it has been well established that hand movements cause a spatially focal increase in high frequency amplitude in the sensorimotor cortex and a spatially distributed decrease in low frequency amplitude (Crone et al., 1998a, 1998b; Miller et al., 2007; Hermes et al., 2012a).

Furthermore, the individual finger movements can be distinguished topographically using the high frequency signals (Miller et al., 2009b; Siero et al., 2014). It is unknown whether these basic physiological changes are maintained after the amputation of a limb.

Several studies have reported that sensorimotor areas reorganize after amputation in humans using transcranial magnetic stimulation (Cohen et al., 1991; Röricht et al., 1999) and fMRI (Elbert et al., 1994; Dettmers et al., 2001; Lotze et al., 2001), and in macaque monkeys using electrical stimulation (Qi et al., 2000) or after lesioning (Kambi et al., 2014). These studies suggest that areas previously related to the

amputated limb can associate with other muscle groups. However, there are several fMRI studies on upper arm amputations that show that some form of hand (Hugdahl et al., 2001; Lotze et al., 2001; Turner et al., 2001; Roux et al., 2003) and finger (Kikkert et al., 2016; Wesselink et al., 2019) representation are preserved in both the motor and sensory cortex, even over longer periods of time. In addition, sensory representations of the hand have been shown to be preserved in patients with tetraplegia using microstimulation of the somatosensory cortex (Flesher et al., 2016; Salas et al., 2018) and EEG studies have shown that ERP responses related to motor inhibition remain intact (Bruno et al., 2019).

Preserved motor physiology would be invaluable for specific clinical purposes such as Brain Computer Interfacing (BCI). Using BCIs, people with paralyses can use the electrophysiological signal from the brain, generated by attempted hand movement, to control communication devices (Vansteensel et al., 2016) or other assistive devices (Benabid et al., 2019). Furthermore, establishing BCI control could potentially help reduce phantom limb-pain (Yanagisawa et al., 2020), it is therefore important to understand the extent to which motor physiology is preserved.

In this study we were provided with a unique opportunity to investigate sensorimotor physiology with ECoG measurements in a patient with an amputated arm. The patient was implanted with an ECoG array for clinical evaluation of phantom limb pain and we measured ECoG signals during attempted finger movements of the contralateral, lost, hand. We investigated whether the typical spatio-temporal organization of hand-movement physiology was preserved and whether information of separate finger representations was retained.

2. Methods

2.1. Participant

A 62-year-old male with a left above-elbow amputation secondary to a snowmobile accident underwent temporary placement of a subdural electrode array for a trial treatment of phantom limb pain by electrical subdural cortical stimulation (Krushelnytskyy et al., 2019). Experimental data were collected during breaks in trials of different electrical stimulation parameters over a period of 10 days. The patient was right-handed and had his left-arm amputated 3 years and 11 months before ECoG grid implantation. The patient reported waking from his initial left mid-forearm amputation with phantom arm and hand pain, and that his pain has persisted since that time. He underwent two additional surgeries, ultimately completing a shoulder disarticulation and full humeral amputation. His pain has resulted in functional impairment and reduced quality of life despite trials of opiate medications, mirror therapy, an intensive pain rehabilitation program, and treatment with an implanted spinal cord stimulator. After the monitoring period, the patient was equipped with a cortical stimulator. At a six months follow up, he reported that the phantom limb pain dropped from 8 to 9/10 severity to a typical range of 5–6/10, and no side effects were reported.

The study was approved by the Institutional Review Board of Mayo Clinic (IRB 15-006530) and the patient provided informed consent to participate in the study, in accordance with the declaration of Helsinki (2013).

2.2. Recordings

An electrode array of 36 circular platinum contacts (AdTech, 6 × 6 electrodes, 2.3 mm exposed diameter, 10 mm inter-electrode distance) embedded in a silastic sheet was surgically placed over the fronto-parietal region, including the sensorimotor cortex (Fig. 1A). Electrodes were localized using a high-resolution CT-scan and projected (Hermes et al., 2010) onto a cortical surface rendering generated from the pre-operative anatomical T1 weighted MRI scan (GE 3T Discovery). During recording, all electrodes were referenced to an inactive subgaleal electrode with the recording surface facing away from the brain. The signals

were amplified and digitalized at 2048 Hz. Upon inspection of the electrode signals, two channels that contained severe noise were excluded from analysis.

2.3. Tasks

The subject was presented with two tasks: an attempted and executed movement task. During the attempted movement task, the subject was asked to attempt finger movements with the (left, contralateral) amputated hand; During the executed movement task the subject was asked to perform finger movement with the (right, ipsilateral) hand on the healthy arm. Both tasks featured the exact same design with 5 s of finger movement and 3 s of rest. The subject was cued via a bedside monitor with a picture of a hand and asked to (attempt to) move one of three fingers: the thumb, index or little finger. Finger movement involved the repeated flexion and extension of the cued finger for the duration of the trial, while no specific instruction was given in regard to the speed of the movement. Each run of a task featured 15 movement cues for each finger, which were presented at random, resulting in 45 randomized trials per run. The subject performed two runs of attempted movement and two runs of executed movement.

2.4. Analysis

The analysis and classification routines were implemented using custom MATLAB (Mathworks inc.) code that is provided alongside this article at: https://osf.io/vmxdn/. Before analysis, the two runs of each task were concatenated and a small number of trials, that showed large artifacts in the signal or in which the patient was distracted, were excluded (2 trials were excluded for attempted movement and 4 trials were excluded for executed movement). The data were re-referenced to the common average by regressing the common average out from each channel.

Since hand and finger movements are known to be controlled by the contralateral hemisphere, the focus of our analyses is mainly on the attempted/phantom movements. However, because there is research that shows that ipsilateral activity does occur during unilateral movement of the hand (Hanakawa et al., 2005; Verstynen et al., 2005; Hlushchuk and Hari, 2006; Horenstein et al., 2009; Diedrichsen et al., 2013) and ipsilateral representations may become more apparent after deafferentation (Valyear et al., 2020), we have - for the sake of completeness - also performed analyses on the ipsilateral executed movements. Furthermore, the behavioral measurements on the intact hand provide a reference for the performance of the invisible hand.

2.5. Spectral power change

The contralateral power changes during attempted hand movement were investigated by extracting an epoch of 1–4 s after cue onset as movement. During executed movement (ipsilateral), the movement epoch was set to start 100 ms before the actual movement of the healthy hand to the end of the actual hand movement based on the concurrent video; 100 ms was subtracted to account for the delay between the cortical signal and initiation of the movement (Evarts, 1973; Cheney and Fetz, 1984; Miller et al., 2009b). An epoch of 2 s before cue onset was considered as rest in both attempted and executed movements. The power spectral density of each epoch was calculated every 1 Hz by Welch's method (Welch, 1967) with a 250 ms window and an overlap of 125 ms. A Hann window (Nuttall, 1981) was applied to each epoch to attenuate the edge effects. Per channel, the resulting power spectra were log10 transformed and normalized to the mean power over all epochs at each frequency. Based on previous ECoG studies into executed and attempted movement we expected frequencies below 30 Hz and above 65 Hz to be most informative (Miller et al., 2007, 2009a, 2009b; Kubánek et al., 2009; Hermes et al., 2012a; Chestek et al., 2013; Blakely et al., 2014; Siero et al., 2014; Bleichner et al., 2016). The high

frequency band (HFB) power was obtained by calculating the average power over 65 Hz to 175 Hz, whereas low frequency band (LFB) power was the average over 15 Hz to 28 Hz. The alpha range (8–13 Hz) has been included in supplementary Fig. 1 for the sake of completeness.

In order to plot the spectral power changes on the rendered brain surface, we calculated the T-statistics for both the HBF and the LFB per channel by testing the power of movement trials against the rest trials. A Bonferroni correction was applied while testing the T-values for significance ($p < .05$).

To visualize the electrophysiological response over time, we filtered each electrode signal using a third-order Butterworth filter for either the high frequencies (HFB, 65–175 Hz), or the low frequencies (LFB, 15–28 Hz). After filtering, the power of the amplitude was calculated using a Hilbert transformation. Trial-epochs, of 2 s before to 7 s after cue onset, were extracted and normalized by subtracting the signal mean power of the 2 s before cue onset from each individual trial. An average across each condition was calculated and smoothed with a moving average window of 1 s.

2.6. Temporal window for finger movement classification

In order to investigate to what degree spatial finger-representations were preserved and distinguishable, single-trial classification was performed on the individual fingers. For executed hand movement, we used the signal when the patient was moving the finger on the healthy hand. However, during attempted finger-movement there is no external behavioral measurement available to assess when (after cue onset) the patient started to attempt the movements, where in time the strongest decodable response occurs and whether such a response is transient or sustained. In order to address these factors, we split the data in two halves. One half was used to explore decodability of the response over time and find the optimal time-window parameters for decoding. Next, these time-window parameters were used in the other half for further decoding analysis. The data was split at random after concatenating the attempted movement runs, while balancing the finger conditions evenly over the two halves. Details on the classification procedure can be found below (under "Classification"); the same procedure was used on both halves of the data

We explored the response over time and optimized it for decoding by applying several different time-windows while decoding the finger-movement, thereby restricting the information available to the classifier. These time-windows differed in size from 250 ms to 5000 ms and in placement from cue onset, ranging from the beginning to the end of the trial.

An optimal time-window for classification was determined by first applying Gaussian smoothing to the classification accuracies over the window size (σ: 2.5) and offset (σ: 0.5) dimensions. Smoothing prevents the selection of parameters with local classification accuracy peaks in the parameter optimization half of the data, and allows for the selection of temporal parameters that are optimal in general. After smoothing, the time-window with the highest classification score was selected, and its offset and size were used for further classification analyses.

2.7. Classification

For classification, the HFB power of the different channels at the trial-epochs were used as features in a Support Vector Machine (SVM) with a linear kernel (Bishop, 2006). The HFB power was calculated per epoch in the same way as described above (i.e. using Welch's method, log10 transformed and averaged over 65–175 Hz), except that the spectra were not normalized. The unnormalized HFB power was used since the SVM maps each input feature to its own (scaled) dimension, and allows us to classify on the movement-epochs alone. We achieved multi-class classification (3 fingers) by applying a one-versus-all classification scheme in which every class is classified against the data of the other classes together and the winner (that is furthest from the

hyperplane) takes all. A leave-one-out cross validation was used and resulted in a classification accuracy score, which is the percentage of trials predicted correctly.

Comparisons to a significance threshold only apply to the half of the data that was used to further investigate the decodability, after applying the optimal time parameters. Classification scores were empirically tested for significance using a Monte Carlo distribution based on 100.000 permutations (Combrisson and Jerbi, 2015). Estimates of the P values were obtained using the equation $p = (r + 1)/(n + 1)$, where n is the number of simulations and r is the number of simulations that produce a classification accuracy greater than or equal to the actual classification accuracy (Davison and Hinkley, 1997).

2.8. Spatial analyses

Searchlight analyses were performed to establish which area on the cortex was most informative for attempted finger movement and how many electrodes (i.e. which grid configurations) would be needed to reliably classify the individual fingers.

The most informative cortical regions to decode attempted finger movements were identified using a random search procedure. During the random search procedure, a subset of 1–36 electrodes was selected at random to classify from. This procedure was repeated 10.000 times and, for each electrode, the average accuracy over all iterations was calculated and z-scored.

Searchlight analyses were performed to identify which anatomical scale of coverage would provide the most information for classification. During the searchlight analyses, a searchlight (i.e. a block of electrodes) was used for classification. The searchlight, with a fixed block size (e.g. 2×2 electrodes) was placed at every possible position within the grid. Afterwards, for each electrode, the average over all the iterations in which that particular electrode was involved was calculated. Searchlight analyses were performed with all possible searchlight sizes and shapes, representing grids of all different sizes ($1 \times 6/6 \times 1$–6×6 electrodes).

3. Results

3.1. A typical electrophysiological motor response occurred upon attempted movement

In order to investigate to what extent the sensorimotor cortex showed typical physiology after deafferentation, we measured ECoG responses in a patient with an amputated arm. The patient reported vivid movements of the amputated hand and could describe in clear fashion how well the different fingers moved during the task. Fig. 1A and B show the electrophysiological differences between attempted movement of the missing hand and rest. During attempted movement, a spatially distributed decrease of LFB power occurred in 91% of electrodes (t-test, $p_{corr.} < 0.05$). Simultaneously, significant focal increases of HFB power were found in 56% of electrodes (t-test, $p_{corr.} < 0.05$), most notably around the primary sensorimotor hand-areas. Strong decreases in power were observed in a narrow range of the lower frequencies (β band, 15–28 Hz), for completeness, supplementary Fig. 1 also illustrates the responses in the alpha range (8–13 Hz). High frequency power increases were distributed over a broad range of higher frequencies (>65 Hz) (Fig. 1B).

During attempted movement there was no behavioral measurement available to determine when - after cue onset – the patient actually starts attempting the movement, nor where in time to expect the physiological response. Fig. 1C and D present the changes in HFB power over time for each of the individual electrodes and the power averaged over all significant electrodes for each condition. A clear peak in HFB power is visible around 1 s second after the cue onset for all fingers.
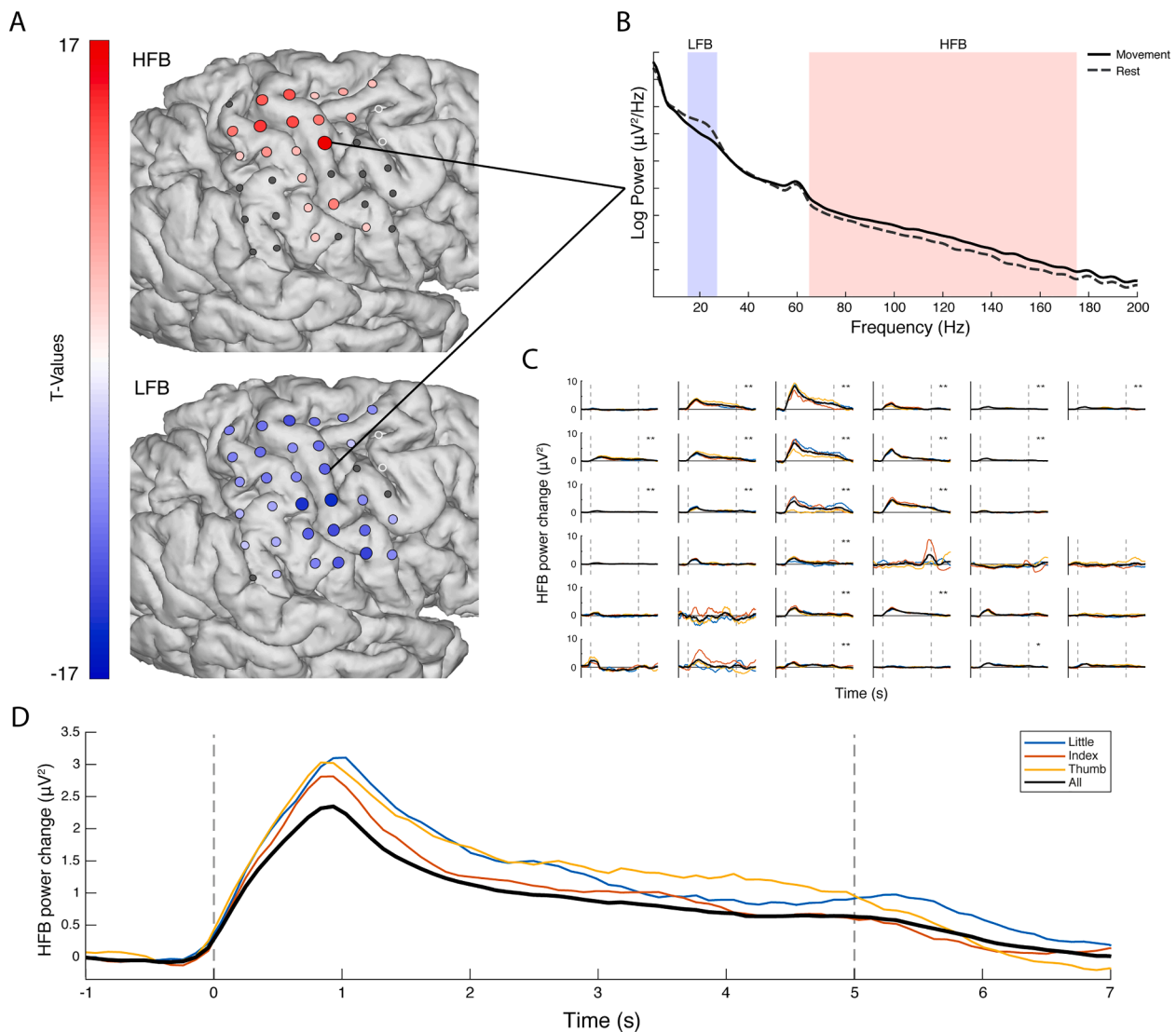
Fig. 1. The electrophysiological response during attempted movement versus rest. (A). The changes in HFB (top, 65–175 Hz) and LFB (bottom, 15–28 Hz) for each grid electrode. Electrodes with a red or blue color had a significant change in band-power, whereas electrodes with an insignificant change in band-power are shown in grey; the two excluded electrodes are shown in white. (B) The power spectra of movement (solid line) and rest (dashed line) for a single electrode. (C) The HFB power changes over time, each graph represents one electrode. The black line represents all fingers, whereas the colored lines represent individual fingers. The two vertical dotted lines indicated the cue on- and offset. (D) The HFB power changes over time were averaged across those electrodes that showed a significant increase for a condition (blue: little, red: index, yellow: thumb, black: all fingers). The black trace has a lower amplitude because a different set of significant electrodes contributed to each trace, with more significant, but lower amplitude electrodes contributing to the black trace. (For interpretation of the references to color in this figure legend, the reader is referred to the web version of this article.)

3.2. Differential electrophysiological responses occur for the three individual fingers

Although each of the individual fingers provided a spatially different electrophysiological response, as shown in Fig. 2, it is difficult to distinguish a clear topographical order.

To investigate whether the representations of the individual fingers were preserved and sufficiently distinguishable we wanted to perform single-trial classification of the individual fingers. However, since there was no behavioral movement information available, we first needed to establish where in time the most information on attempted finger movement was present. By restricting the classification to the information within specific time-windows we could explore where in time the most information about attempted finger movement resided. Fig. 3 shows the classification accuracies based on the HFB power within a specific window of time, ranging from 250 ms to 5000 ms, placing the window at different moments between the cue onset (t = 0 ms) and

offset (t = 5000 ms).

Smaller time windows (<750 ms) seem to provide less good decoding accuracies (0%–50%) in comparison to medium (750–2500 ms) or larger time-windows. Medium-sized windows can perform reasonably well (60%–80%) depending on their offset in time. Window sizes of about 2500 ms to 5000 ms performed well overall (>~70%). In terms of window offset, the highest classifying windows take information from the beginning of the trial, regardless of window size. After Gaussian smoothing (Fig. 3C) of the classification results, the optimal window (i.e. the highest classification score) was found at a width of 3000 ms at 1950 ms (window center) after cue onset, which converts to an epoch window from 450 ms to 3450 ms after cue onset. The remainder of the results are based on this epoch and are performed on the half of the data that was not used for parameter optimization.

The second half of the data showed that the classification accuracy of attempted finger movements based on the spatial features of the HFB power was significant at 93% (above 45% chance level calculated with
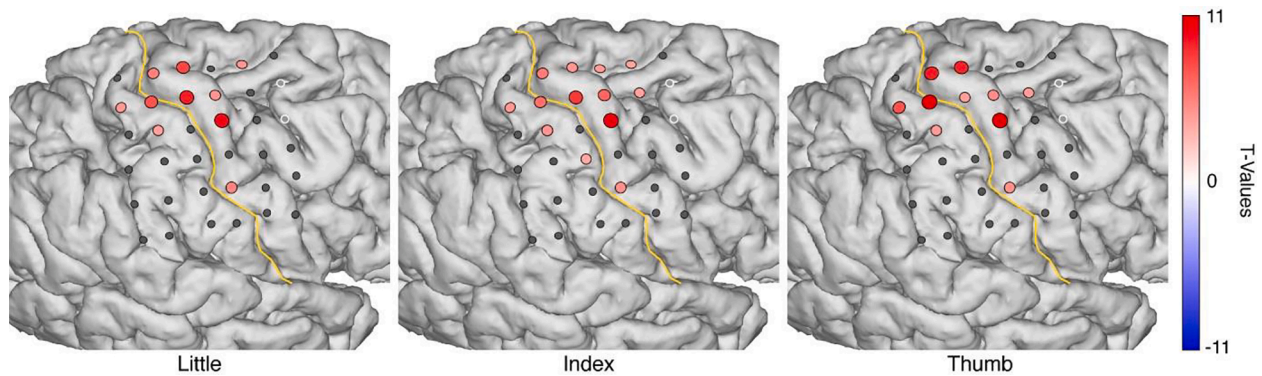
Fig. 2. The HFB power changes upon attempted movement of each individual finger. Electrodes with a significant change in HFB band-power are shown in red, whereas electrodes with an insignificant HFB change are shown in grey, the two electrodes that were excluded are shown in white. The yellow line represents the central sulcus. (For interpretation of the references to color in this figure legend, the reader is referred to the web version of this article.)
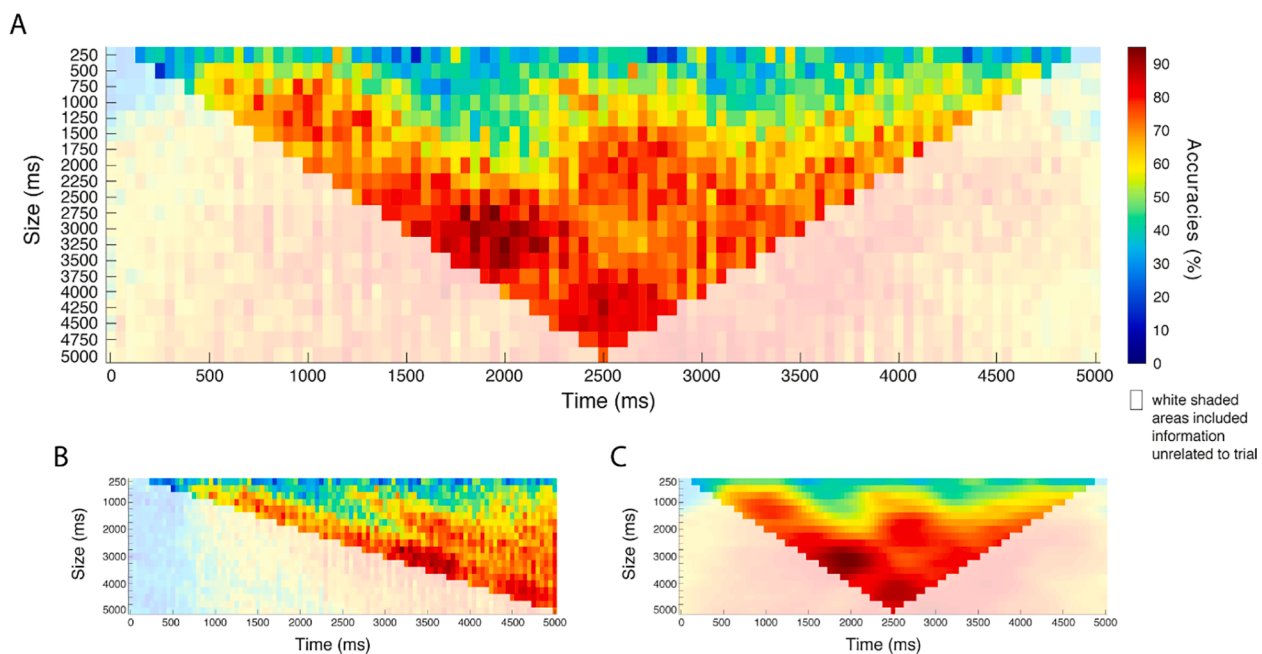

Fig. 3. The classification accuracies at different window sizes (y-axes) and offsets from cue onset (x-axes), based on half of the data (~45 trials). (A) The x-axis indicates the center of each window. (B) The same plot shown, but with the x-axis indicating the right of each window, such that each time point includes the information present before that time. (C) Shows the classification accuracies smoothed with a Gaussian filter (offset σ: 0.5, size σ: 2.5). The white-shaded regions in each graph indicate the classification accuracies in which the window included information unrelated to the trial (i.e. rest before or after the trial).

Monte-Carlo simulation; one-sided, $p < .05$). The sensitivity values for each of the individual fingers (Little: 87%, Index: 93% and Thumb: 100%), shown in Fig. 4, were also significantly above chance (one sided, each p < .05).

3.3. Topographical organization of attempted hand movement information

For all of the finger movements we investigated where on the cortex the related activity was located. Figs. 1 and 2 already showed that most of the HFB power changes related to attempted movement occur around the hand and arm region of the pre and post central gyrus. Significant HFB changes extended beyond pre and post central gyrus to more anterior premotor regions as well. The random search classification results in Fig. 5C confirm that most information indeed resides in S1 and M1, specifically in areas of the pre and post central gyrus that are well known to represent hand and finger movements (Penfield and Boldrey, 1937).

To test the spatial extent of finger movement information, searchlight analyses with different types of grid configurations were performed (Fig. 5A and B). Grid configurations with one or two electrodes tended to perform more poorly (~60%) compared to grids that include at least 3 electrodes (>60%). For electrodes strips (i.e. grids that have multiple electrodes only in one dimension), the orientation of the grid becomes important. Grids with 3–6 electrodes that are placed along the superior-inferior axis perform much better at >70% than grids are oriented on the anterior-posterior axis (at ~60%). This coincides with the topographical organization of the different fingers on the cortex, which is more superior-inferior oriented than anterior-posterior (Dechent and Frahm, 2003; Miller et al., 2009b; Siero et al., 2014; Schellekens et al., 2018; Huber et al., 2020). In accordance with the most informative area in Fig. 5C, grids perform best when 2–3 electrodes wide and at least 2–3 electrodes high, in order to cover enough area of the brain to include the most informative electrodes. Given the inter-electrode distance of 10 mm, the minimum required grid size to obtain a good (>=80%) classification would be around 13 mm × 13 mm (2 × 2 electrodes).

Fig. 4. Confusion matrix with the classification scores of the individual fingers. Each column represents the finger of which movement was attempted. The rows represent how each of those finger movements was classified.
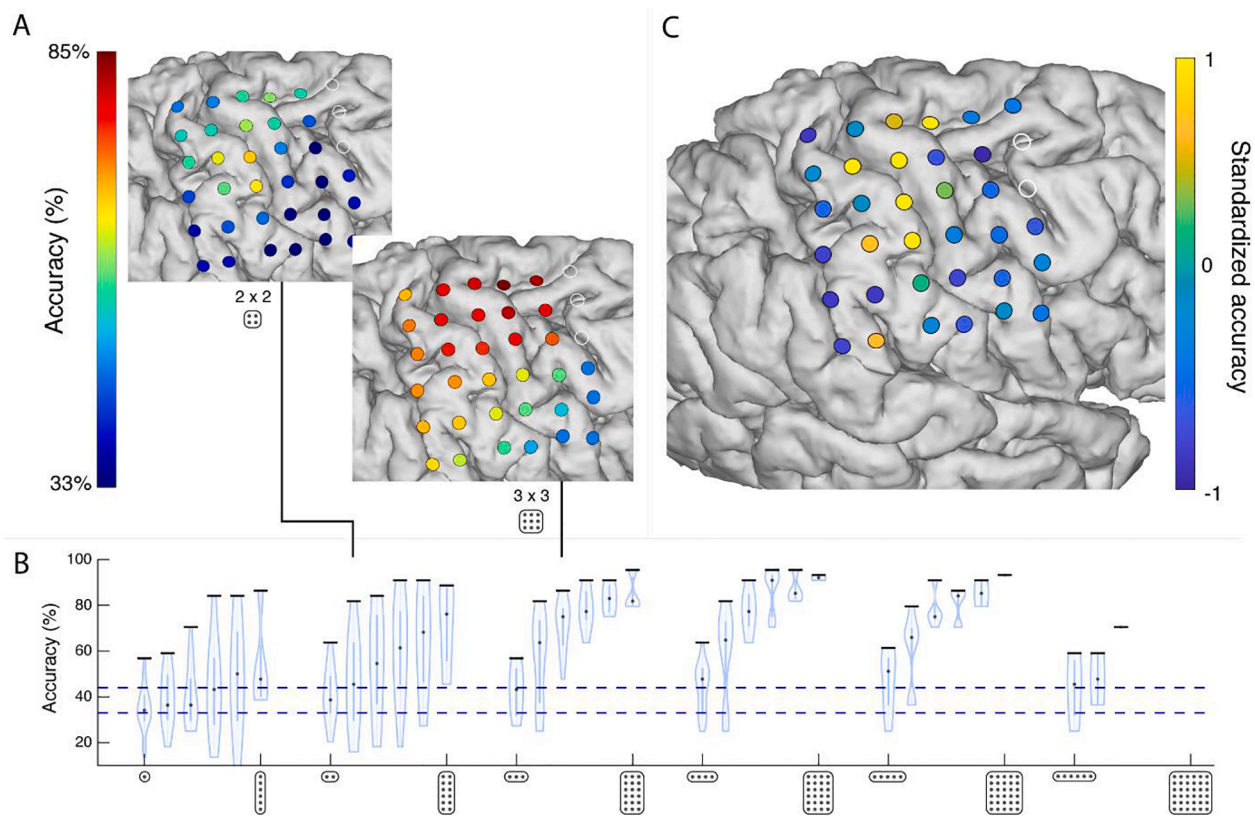

Fig. 5. The spatial distribution of information. (A) Searchlight classification maps of searchlight with 2 × 2 (top) and 3 × 3 electrodes (bottom). (B) The classification results of the different searchlights, ranging from 1 × 6 to 6 × 6 grids in two directions (superior-inferior, anterior-posterior). Each violin plot represents the searchlight results with a specific grid configuration. The violin represents the distribution of the classification accuracies at the different searchlight positions within the grid, with a black horizontal bar to indicate the searchlight position that classified the highest. The lower dotted blue line shows the chance level at 33%, while the upper blue line indicates the threshold of 45% above which the decoding accuracy was significant. Note that, for the larger searchlight grids, virtual placements were limited or not possible due to overlap with the bad electrodes. (C) Most informative electrodes, identified by a random search classification on 10.000 subsets of electrodes. (For interpretation of the references to color in this figure legend, the reader is referred to the web version of this article.)
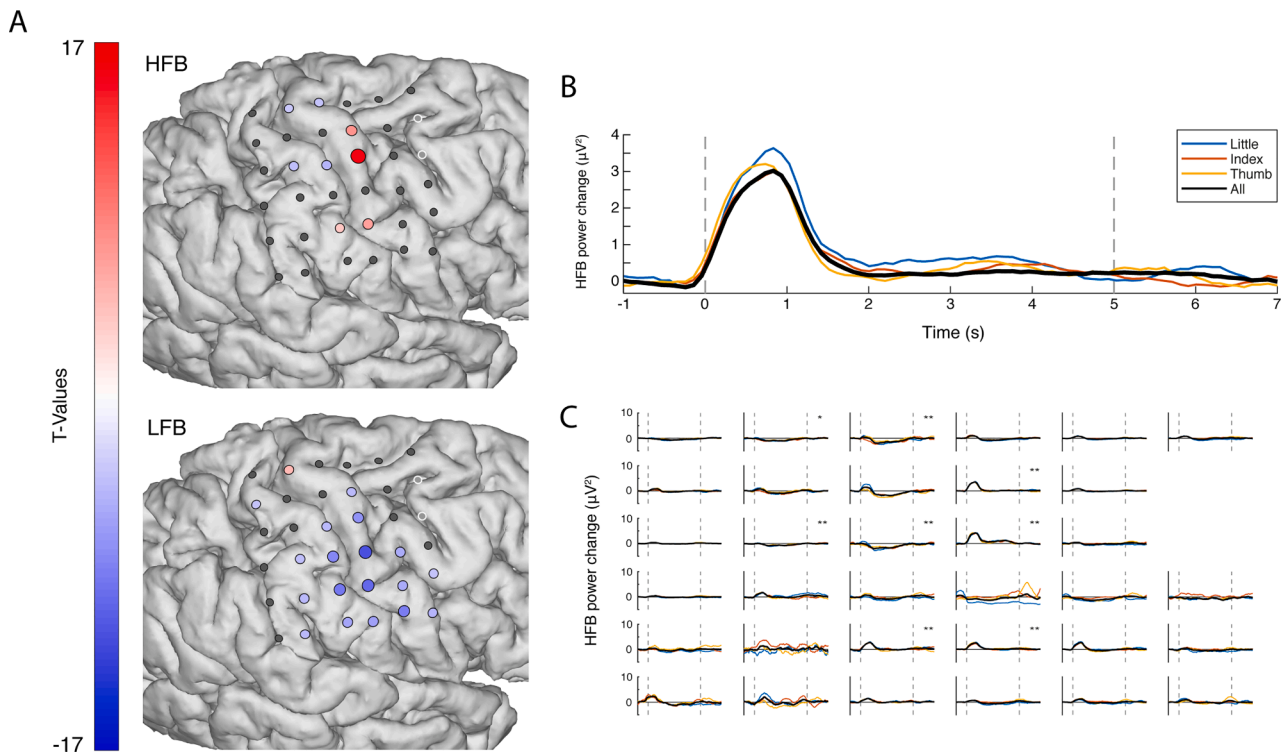
Fig. 6. The, ipsilateral, electrophysiological response of executed movement versus rest. (A) The changes in HFB (top, 65–175 Hz) and LFB power (bottom, 15–28 Hz) for each grid electrode. Electrodes with a red or blue color showed a significant change in band-power, whereas electrodes with an insignificant change in band-power are shown in grey; the two excluded electrodes are shown in white. (B) HFB power changes over time averaged across those electrodes that showed a significant positive increase. The black line represents all fingers, whereas the colored lines represent individual fingers. The two vertical dotted lines indicated the cue on- and offset. (C) The HFB power changes over time, each graph represents one electrode. (For interpretation of the references to color in this figure legend, the reader is referred to the web version of this article.)

3.4. Ipsilateral finger representations

In addition to attempted movement, the patient also performed runs of executed hand movements with the healthy, ipsilateral, hand. Frame-perfect video annotations were used to quantify the movement of the healthy hand. An average delay of 0.44 s (std: 0.09) occurred between the cue onset and actual start of the movement. The patient moved his hand for about 3.69 s (std: 0.53) on average over all trials, with about 3–5 flexions of the finger per trial.

Only a few channels on the hand-area showed a strong ipsilateral increase in HFB power during executed movement, whereas some other channels showed a smaller, yet significant, ipsilateral decrease in HFB power (Fig. 6). An ipsilateral distributed decrease in LFB was found, but was less spread out over the cortex compared to attempted movement. The HFB power for executed movement showed a transient response with a temporal peak between 0.5 s and 1 s, in line with the behavioral start of the hand movement and slightly earlier than the HFB peak in attempted movement at 1 s.

Classification was performed on the ipsilateral response to the movement of the healthy hand. Based on the HFB power of all electrodes, finger movements could be classified with an accuracy of 56%.

4. Discussion

In order to understand whether somatomotor physiology is preserved after deafferentation, we investigated the contralateral electrophysiological responses of attempted finger movements in a single patient with an upper-arm amputation. With attempted movement, a spatially-focal increase was found in broadband high-frequency ranges (65–175 Hz) over the hand-area of the primary sensorimotor cortex. A spatially distributed decrease was found in the lower frequency bands

(15–28 Hz).

The electrophysiological response in our patient with an amputated arm is similar to what is seen in many previous studies that have investigated ECoG spectral power changes during finger movements. These studies show typical physiological responses, with a localized high frequency increase and a distributed low frequency decrease (Crone et al., 1998a, 1998b; Miller et al., 2007). Finger somatotopy is represented in both the M1 and S1 and can be decoded from high frequency activity (Kubánek et al., 2009; Miller et al., 2009b; Siero et al., 2014; Branco et al., 2017). The similarity between our results and those in healthy people suggests that the motor physiology of the hand is retained. Still, it is important to understand whether this typical physiology is retained in different patient populations.

Studies that investigated the motor electrophysiology in patients with locked-in-syndrome (i.e. ALS, PLS or brainstem-stroke) using EEG, MEG or permanent ECoG implants found similar results. In these patients, a robust HFB response was retained (Freudenburg et al., 2019). Whether and/or how the LFB response was affected varied between studies. Some studies observed robust low frequency power decreases in patients with ALS and/or PLS (Bai et al., 2010; Riva et al., 2012; Proudfoot et al., 2017). Other studies reported reduced power decreases in ALS (Kasahara et al., 2012), or more variability between patients with ALS, tetraplegia and brainstem stroke, with only some patients showing robust low frequency power decreases (Höhne et al., 2014; Freudenburg et al., 2019). These studies suggest that whether low frequency power decreases are retained depends on the disease (progression) and the influence of closed-loop feedback training. Here we have observed that there are strong and significant low frequency power decreases during attempted movement in a patient with an amputated arm.

The HFB response of attempted movement was both transient and sustained, similar to what was found in research on continuous/repeated

executed finger movements (Hermes et al., 2012b; Siero et al., 2013). For attempted movement, the HFB power peaked at ~1 s after cue onset and returned gradually back to baseline during the remainder of the trial. Part of the latency between the cue onset and the peak of the cortical response can be explained by the lag between the interpretation of the cue and movement initiation, which in the executed movements of the patient already accounted for ~0.5 s. Another factor that could have contributed to this ~1 s latency may be related to the fact that motor imagery can be demanding in terms of mental fatigue and effort (Papadelis et al., 2007; Jacquet et al., 2020). In terms of decoding, both the transient and the sustained responses contained information about finger movements. The classifications of attempted finger movement over time confirmed that most information (i.e. the highest classification accuracies) was found around the peak of the response at 1 s after cue presentation. The classification accuracies were more variable when including only the sustained response. However, larger time-windows (>2500 ms) that included both the transient and sustained responses yielded higher classification accuracies than smaller windows (<2500 ms), implying that the inclusion of (part of) the sustained response can contribute to the decodability.

Each individual finger resulted in a strong HFB response in the hand-region of the sensorimotor cortex. Although each of the fingers elicited a different HFB response pattern, no clear topographical representation of the fingers was found. Regardless, using support vector machine learning, we were able to decode the attempted movement of three individual fingers significantly at a classification accuracy of 93% (well above the 33% chance level). Which is similar to the decoding accuracies of executed movement of the fingers (Kubánek et al., 2009; Chestek et al., 2013). Attempted movements of the thumb could be decoded at 100% accuracy, however the index and little finger were less discriminable with sensitivity values of respectively 93% and 87%. Such decoding accuracies confirm that individual finger representations in the cortex are retained and can be distinguished in a patient with an amputated arm. These results align with earlier fMRI research on patients with long term upper arm amputations (Kikkert et al., 2016; Bruurmijn et al., 2017; Wesselink et al., 2019), while other fMRI studies have shown displacement of the cortical activation into the deafferented motor and somatosensory areas during lip (Lotze et al., 2001), chin (Elbert et al., 1994) and face/shoulder movement (Dettmers et al., 2001). It is possible that the cortical representations of other body parts invade the cortical regions of an amputated limb, which would warrant further investigation. However, studies in the visual cortex have shown only a limited ability for the primary cortex to reorganize (Smirnakis et al., 2005). Our research similarly demonstrates that, while it is possible that representations co-exist, the electrophysiological signals related to finger representation of the missing hand are at least largely retained and not replaced by other functions.

In contrast to tetraplegic or locked-in-patients, there are several important aspects to consider in patients with an amputated limb. For one, attempted movements by patients with an amputated arm could be considered as phantom movements, where potential residual output to muscles and input from nerve endings in the stump may play a role. In addition, this patient experienced phantom pain, and there may be a link between this pain and the neurophysiological responses we observed. Phantom pains are believed to arise from maladaptive cortical reorganization invading the cortical region of the missing limb (Yang et al., 1994; Flor et al., 2006), which is supported by several studies that show a (positive) relation between the displacement of cortical activity and phantom pains (Flor et al., 1995; Birbaumer et al., 1997; Dettmers et al., 2001; Karl et al., 2001; Lotze et al., 2001; Diers et al., 2010). As such, various mirror or hand imagery therapies aimed towards the re-engagement of the invaded cortical areas have been developed and shown to reduce phantom pains (Giraux and Sirigu, 2003; Moseley, 2006; Brodie et al., 2007; Chan et al., 2007; MacIver et al., 2008). However, recent studies have shown that people with chronic pain can also exhibit greater activity during phantom movement (Makin et al.,

2013; Kikkert et al., 2018). Also, a study with a large sample of phantom limb patients did not report a relationship between phantom pain and cortical reorganization (Makin et al., 2015). It appears that the relation between the chronic phantom pain and retained physiology is more complex and the exact workings are still debated (Flor et al., 2013; Makin and Flor, 2020). Based on our experiment, it is not possible to draw conclusions on the effect of phantom pains on the representations of the missing hand. However, taking into account that, first, there are a number of fMRI studies that include patients with upper arm amputations that still have representations of their missing hand upon attempted/phantom movement while having no phantom limb pains (Diers et al., 2010) or low to medium phantom limb pains (Bruurmijn et al., 2017; Kikkert et al., 2018). Second, studies into tetraplegia and stroke patients have shown that even without these "phantom" factors and without any peripheral information, finger and hand representations are preserved in primary sensory and motor areas (Yanagisawa et al., 2012; Flesher et al., 2016; Salas et al., 2018). Therefore, it seems likely that the increased high frequency activity, decreased low frequency activity and decodable finger movements are not merely driven by the stump or phantom limb pains. In addition, previous MEG research that uses a (virtual) prosthesis (Yanagisawa et al., 2016, 2020), suggests that the intact hand representations in the phantom cortex may be actively used in a BCI and could potentially reduce phantom limb pain.

In BCI applications, devices are often controlled with signals from the sensorimotor cortex using attempted movements (Collinger et al., 2013; Bouton et al., 2016; Vansteensel et al., 2016; Benabid et al., 2019). Our data showed that we could decode finger movements after deafferentation, suggesting that these motor programs are retained by some degree and these signals can also be used to control a BCI. Understanding which signal properties allow for reliable decoding and BCI control is essential for these applications. Temporally, different parts of the electrophysiological signals can be included, but a tradeoff can occur between the speed of decoding and classification accuracy. A smaller window could allow for faster and more subsequent classifications, but could go at the expense of classification accuracy. Our data suggest that shorter (e.g. 1000 ms) time windows may already provide a good accuracy (~80%) for decoding 3 fingers, while larger windows (e.g. 3000 ms) will further improve accuracy (>90%). Patients may be able to use such short time windows, as one study in a patient with ALS already showed that movement versus rest can be decoded using a 1 sec window (Vansteensel et al., 2016). Understanding how well movement activity is retained after deafferentation may have implications for BCIs in patients with paralysis, as well as an amputated limb, as BCIs may reduce phantom limb pain (Yanagisawa et al., 2020).

Attempted movement after loss of function is different from imagined movements in healthy people, a distinction that is of particular importance for implanted BCIs. It has been debated whether motor imagery representation overlaps with overt movement in brain surface recordings (Miller et al., 2010; Hermes et al., 2011), and whether motor imagery is a good approximation of attempted movement after limb loss or paralysis. One would intuitively expect that, in the case of a lost limb, the native map of representation would either be retained, or generally degrade. This patient's map shows that somatotopic distinction is retained several years after limb loss. Some types of motor imagery in healthy individuals may thus not be a good general approximation or motor representations after limb loss or paralysis for implanted BCIs.

An additional point of importance for BCIs is the electrode grid design and extent of cortical coverage, which can have a strong influence on BCI performance (Vansteensel et al., 2016; van den Boom et al., 2021). Our results show that most information about attempted movement is located on the hand-region of the primary motor and sensory cortex. In terms of cortical coverage, considering an inter-electrode distance of 10 mm, a good (>80%) classification accuracy can already be achieved with as little as 2x2 electrodes (13 mm × 13 mm) placed over the primary sensorimotor cortex. More electrodes could provide up to ~90% classification accuracy.

Finger movement activity on the ipsilateral cortex of the intact hand could be decoded, but less accurately compared to decoding the contralateral attempted finger movements, suggesting that the contralateral, phantom limb, still has a stronger representation compared to the ipsilateral hand. Only a few channels showed power increases during ipsilateral movements, while some electrodes also showed significant high frequency power decreases. Whether previous ECoG studies show similar ipsilateral high frequency power decreases during executed hand movements is less clear (Zanos et al., 2008). However, ipsilateral decreases in sensorimotor activity during hand movement in healthy subjects have been observed in the fMRI BOLD signal (Hlushchuk and Hari, 2006; Diedrichsen et al., 2013). TMS studies similarly show evidence for contralateral inhibition (Talelli et al., 2008a, 2008b). The ipsilateral decreases in high frequency power we observed with ECoG may thus potentially be related to inhibition resulting from activity of the contralateral hemisphere, or to some reorganization of function after the injury (as has been seen with patients after perinatal hemispheric stroke; Miller et al., 2011).

5. Conclusion

This case study shows that the electrophysiology of attempted hand movement is preserved in the sensorimotor cortex after deafferentation of an amputated hand, with a typical focal increase of HFB power over the hand region and a more distributed decrease in LFB. Attempted finger movements provided a transient HFB peak around 1 s after cue onset, followed by a sustained HFB response. Classification analyses confirm that most decodable information on the finger movement can be found around this peak. Furthermore, HFB power can be used to decode finger movements with high (>90%) accuracy. Optimal decoding could be achieved based on the first 1–3 s of the signal and would only require 13–13 mm of cortical coverage. Our results demonstrate that the sensorimotor electrophysiology remains largely intact after long term (3 years and 11 months) amputation and therefore remains a viable region for BCIs that use the decoding of hand-gestures for control.

CRediT authorship contribution statement

Max van den Boom: Conceptualization, Methodology, Validation, Software, Formal analysis, Writing - original draft, Writing - review & editing. **Kai J. Miller:** Conceptualization, Resources, Writing - original draft. **Nicholas M. Gregg:** Resources, Writing - review & editing. **Gabriela Ojeda Valencia:** Validation, Data curation. **Kendall H. Lee:** Resources. **Thomas J. Richner:** Conceptualization, Resources. **Nick F. Ramsey:** Supervision. **Greg A. Worrell:** Conceptualization, Resources, Writing - review & editing. **Dora Hermes:** Conceptualization, Methodology, Validation, Investigation, Writing - original draft, Writing - review & editing, Supervision, Funding acquisition.

and interpretation of data; in the writing of the report; and in the decision to submit the paper for publication.

Appendix A. Supplementary data

Supplementary data to this article can be found online at https://doi.org/10.1016/j.nicl.2021.102728.

References

Bai, O., Lin, P., Huang, D., Fei, D.Y., Floeter, M.K., 2010. Towards a user-friendly brain-computer interface: initial tests in ALS and PLS patients. Clin. Neurophysiol. 121, 1293–1303.

Benabid, A.L., Costecalde, T., Eliseyev, A., Charvet, G., Verney, A., Karakas, S., Foerster, M., Lambert, A., Morinière, B., Abroug, N., Schaeffer, M.C., Moly, A., Sauter-Starace, F., Ratel, D., Moro, C., Torres-Martinez, N., Langar, L., Oddoux, M., Polosan, M., Pezzani, S., Auboiroux, V., Aksenova, T., Mestais, C., Chabardes, S., 2019. An exoskeleton controlled by an epidural wireless brain–machine interface in a tetraplegic patient: a proof-of-concept demonstration. Lancet Neurol. 18, 1112–1122.

Birbaumer, N., Lutzenberger, W., Montoya, P., Larbig, W., Unertl, K., Töpfner, S., Grodd, W., Taub, E., Flor, H., 1997. Effects of regional anesthesia on phantom limb pain are mirrored in changes in cortical reorganization. J. Neurosci. 17, 5503–5508.

Bishop, C.M., 2006. Machine Learning and Pattern Recoginiton, Information Science and Statistics. Springer-Verlag, New York.

Blakely, T.M., Olson, J.D., Miller, K.J., Rao, R.P.N., Ojemann, J.G., 2014. Neural correlates of learning in an electrocorticographic motor-imagery brain-computer interface. Brain-Comput. Interfaces 1, 147–157.

Bleichner, M.G., Freudenburg, Z.V., Jansma, J.M., Aarnoutse, E.J., Vansteensel, M.J., Ramsey, N.F., 2016. Give me a sign: decoding four complex hand gestures based on high-density ECoG. Brain Struct. Funct. 221, 203–216.

Bouton, C.E., Shaikhouni, A., Annetta, N.V., Bockbrader, M.A., Friedenberg, D.A., Nielson, D.M., Sharma, G., Sederberg, P.B., Glenn, B.C., Mysiw, W.J., Morgan, A.G., Deogaonkar, M., Rezai, A.R., 2016. Restoring cortical control of functional movement in a human with quadriplegia. Nature 533, 247–250.

Branco, M.P., Freudenburg, Z.V., Aarnoutse, E.J., Bleichner, M.G., Vansteensel, M.J., Ramsey, N.F., 2017. Decoding hand gestures from primary somatosensory cortex using high-density ECoG. Neuroimage 147, 130–142.

Brodie, E.E., Whyte, A., Niven, C.A., 2007. Analgesia through the looking-glass? A randomized controlled trial investigating the effect of viewing a 'virtual' limb upon phantom limb pain, sensation and movement. Eur. J. Pain 11, 428–436.

Bruno, V., Ronga, I., Fossataro, C., Capozzi, F., Garbarini, F., 2019. Suppressing movements with phantom limbs and existing limbs evokes comparable electrophysiological inhibitory responses. Cortex 117, 64–76.

Bruurmijn, M.L.C.M., Pereboom, I.P.L., Vansteensel, M.J., Raemaekers, M.A.H., Ramsey, N.F., 2017. Preservation of hand movement representation in the sensorimotor areas of amputees. Brain 140, 3166–3178.

Chan, B.L., Witt, R., Charrow, A.P., Magee, A., Howard, R., Pasquina, P.F., Heilman, K.M., Tsao, J.W., 2007. Mirror therapy for phantom limb pain. N. Engl. J. Med. 357, 2206–2207.

Cheney, P.D., Fetz, E.E., 1984. Corticomotoneuronal cells contribute to long-latency stretch reflexes in the rhesus monkey. J. Physiol. 349, 249–272.

Chestek, C.A., Gilja, V., Blabe, C.H., Foster, B.L., Shenoy, K.V., Parvizi, J., Henderson, J.M., 2013. Hand posture classification using electrocorticography signals in the gamma band over human sensorimotor brain areas. J. Neural Eng. 10, 26002–26013.

Cohen, L.G., Bandinelli, S., Findley, T.W., Hallett, M., 1991. Motor reorganization after upper limb amputation in man: a study with focal magnetic stimulation. Brain 114, 615–627.

Collinger, J.L., Wodlinger, B., Downey, J.E., Wang, W., Tyler-Kabara, E.C., Weber, D.J., McMorland, A.J.C., Velliste, M., Boninger, M.L., Schwartz, A.B., 2013. High-performance neuroprosthetic control by an individual with tetraplegia. Lancet 381, 557–564.

Combrisson, E., Jerbi, K., 2015. Exceeding chance level by chance: The caveat of theoretical chance levels in brain signal classification and statistical assessment of decoding accuracy. J. Neurosci. Methods 250, 126–136.

Crone, N.E., Miglioretti, D.L., Gordon, B., Lesser, R.P., 1998. Functional mapping of human sensorimotor cortex with electrocorticographic spectral analysis: II. Event-related synchronization in the gamma band. Brain 121, 2301–2315.

Crone, N.E., Miglioretti, D.L., Gordon, B., Sieracki, J.M., Wilson, M.T., Uematsu, S., Lesser, R.P., 1998. Functional mapping of human sensorimotor cortex with electrocorticographic spectral analysis: I. Alpha and beta event-related desynchronization. Brain 121, 2271–2299.

Davison, A.C., Hinkley, D V. 1997. Bootstrap Methods and their Application, Bootstrap Methods and their Application.

Dechent, P., Frahm, J., 2003. Functional somatotopy of finger representations in human primary motor cortex. Hum. Brain Mapp. 18, 272–283.

Dettmers, C., Adler, T., Rzanny, R., Van Schayck, R., Gaser, C., Weiss, T., Miltner, W.H., Brückner, L., Weiller, C., 2001. Increased excitability in the primary motor cortex and supplementary motor area in patients with phantom limb pain after upper limb amputation. Neurosci. Lett. 307, 109–112.

Diedrichsen, J., Wiestler, T., Krakauer, J.W., 2013. Two distinct ipsilateral cortical representations for individuated finger movements. Cereb. Cortex 23, 1362–1377.

Diers, M., Christmann, C., Koeppe, C., Ruf, M., Flor, H., 2010. Mirrored, imagined and executed movements differentially activate sensorimotor cortex in amputees with and without phantom limb pain. Pain 149, 296–304.

Elbert, T., Flor, H., Birbaumer, N., Knecht, S., Hampson, S., Larbig, W., Taub, E., 1994. Extensive reorganization of the somatosensory cortex in adult humans after nervous system injury. NeuroReport 5, 2593–2597.

Evarts, E.V., 1973. Motor cortex reflexes associated with learned movement. Science (80-.). 179, 501–503.

Flesher, S.N., Collinger, J.L., Foldes, S.T., Weiss, J.M., Downey, J.E., Tyler-Kabara, E.C., Bensmaia, S.J., Schwartz, A.B., Boninger, M.L., Gaunt, R.A., 2016. Intracortical microstimulation of human somatosensory cortex. Sci. Transl. Med. 8, 361ra141-361ra141.

Flor, H., Diers, M., Andoh, J., 2013. The neural basis of phantom limb pain. Trends Cogn. Sci.

Flor, H., Elbert, T., Knecht, S., Wienbruch, C., Pantev, C., Birbaumers, N., Larbig, W., Taub, E., 1995. Phantom-limb pain as a perceptual correlate of cortical reorganization following arm amputation. Nature 375, 482–484.

Flor, H., Nikolajsen, L., Jensen, T.S., 2006. Phantom limb pain: a case of maladaptive CNS plasticity? Nat. Rev. Neurosci.

Freudenburg, Z.V., Branco, M.P., Leinders, S., Vijgh, B.H. va. der., Pels, E.G.M., Denison, T., Berg, L.H. va. den, Miller, K.J., Aarnoutse, E.J., Ramsey, N.F., Vansteensel, M.J., 2019. Sensorimotor ECoG signal features for BCI control: a comparison between people with locked-in syndrome and able-bodied controls. Front Neurosci 13.

Giraux, P., Sirigu, A., 2003. Illusory movements of the paralyzed limb restore motor cortex activity. In: NeuroImage. Academic Press Inc., pp. S107–S111.

Hanakawa, T., Parikh, S., Bruno, M.K., Hallett, M., 2005. Finger and face representations in the ipsilateral precentral motor areas in humans. J. Neurophysiol. 93, 2950–2958.

Hermes, D., Miller, K.J., Noordmans, H.J., Vansteensel, M.J., Ramsey, N.F., 2010. Automated electrocorticographic electrode localization on individually rendered brain surfaces. J. Neurosci. Methods 185, 293–298.

Hermes, D., Miller, K.J., Vansteensel, M.J., Aarnoutse, E.J., Leijten, F.S.S., Ramsey, N.F., 2012a. Neurophysiologic correlates of fMRI in human motor cortex. Hum. Brain Mapp. 33, 1689–1699.

Hermes, D., Siero, J.C.W., Aarnoutse, E.J., Leijten, F.S.S., Petridou, N., Ramsey, N.F., 2012b. Dissociation between neuronal activity in sensorimotor cortex and hand movement revealed as a function of movement rate. J. Neurosci. 32, 9736–9744.

Hermes, D., Vansteensel, M.J., Albers, A.M., Bleichner, M.G., Benedictus, M.R., Mendez Orellana, C., Aarnoutse, E.J., Ramsey, N.F., 2011. Functional MRI-based identification of brain areas involved in motor imagery for implantable brain-computer interfaces. J. Neural Eng.

Hlushchuk, Y., Hari, R., 2006. Transient suppression of ipsilateral primary somatosensory cortex during tactile finger stimulation. J. Neurosci. 26, 5819–5824.

Höhne, J., Holz, E., Staiger-Sälzer, P., Müller, K.R., Kübler, A., Tangermann, M., 2014. Motor imagery for severely motor-impaired patients: Evidence for brain-computer interfacing as superior control solution. PLoS ONE 9.

Horenstein, C., Lowe, M.J., Koenig, K.A., Phillips, M.D., 2009. Comparison of unilateral and bilateral complex finger tapping-related activation in premotor and primary motor cortex. Hum. Brain Mapp. 30, 1397–1412.

Huber, L., Finn, E.S., Handwerker, D.A., Bönstrup, M., Glen, D.R., Kashyap, S., Ivanov, D., Petridou, N., Marrett, S., Goense, J., Poser, B.A., Bandettini, P.A., 2020. Sub-millimeter fMRI reveals multiple topographical digit representations that form action maps in human motor cortex. Neuroimage 208, 116463.

Hugdahl, K., Rosén, G., Ersland, L., Lundervold, A., Smievoll, A.I., Barndon, R., Thomsen, T., 2001. Common pathways in mental imagery and pain perception: An fMRI study of a subject with an amputated arm. Scand. J. Psychol. 42, 269–275.

Jacquet, T., Lepers, R., Poulin-Charronnat, B., Bard, P., Pfister, P., Pageaux, B., 2020. Mental fatigue induced by prolonged motor imagery increases perception of effort and the activity of motor areas. Neuropsychologia 150.

Kambi, N., Halder, P., Rajan, R., Arora, V., Chand, P., Arora, M., Jain, N., 2014. Large-scale reorganization of the somatosensory cortex following spinal cord injuries is due to brainstem plasticity. Nat. Commun. 5, 1–10.

Karl, A., Birbaumer, N., Lutzenberger, W., Cohen, L.G., Flor, H., 2001. Reorganization of motor and somatosensory cortex in upper extremity amputees with phantom limb pain. J. Neurosci. 21, 3609–3618.

Kasahara, T., Terasaki, K., Ogawa, Y., Ushiba, J., Aramaki, H., Masakado, Y., 2012. The correlation between motor impairments and event-related desynchronization during motor imagery in ALS patients. BMC Neurosci. 13, 1–10.

Kikkert, S., Johansen-Berg, H., Tracey, I., Makin, T.R., 2018. Reaffirming the link between chronic phantom limb pain and maintained missing hand representation. Cortex 106, 174–184.

Kikkert, S., Kolasinski, J., Jbabdi, S., Tracey, I., Beckmann, C.F., Berg, H.J., Makin, T.R., 2016. Revealing the neural fingerprints of a missing hand. Elife 5.

Krushelnytskyy, M.D., Carlstrom, L.P., Klassen, B.T., Lundstrom, B.N., Paek, S. (Brian), Lavrov, I.A., Stead, S.M., Sandroni, P., Lee, K.H., 2019. Chronic subdural cortical stimulation for phantom limb pain: report of a series of two cases. Acta Neurochir (Wien) 161, 925–934.

Kubánek, J., Miller, K.J., Ojemann, J.G., Wolpaw, J.R., Schalk, G., 2009. Decoding flexion of individual fingers using electrocorticographic signals in humans. J. Neural Eng. 6.

Lotze, M., Flor, H., Grodd, W., Larbig, W., Birbaumer, N., 2001. Phantom movements and pain an fMRI study in upper limb amputees. Brain 124, 2268–2277.

MacIver, K., Lloyd, D.M., Kelly, S., Roberts, N., Nurmikko, T., 2008. Phantom limb pain, cortical reorganization and the therapeutic effect of mental imagery. Brain 131, 2181–2191.

Makin, T.R., Flor, H., 2020. Brain (re)organisation following amputation: Implications for phantom limb pain. Neuroimage 218.

Makin, T.R., Scholz, J., Filippini, N., Henderson Slater, D., Tracey, I., Johansen-Berg, H., 2013. Phantom pain is associated with preserved structure and function in the former hand area. Nat. Commun. 4, 1–8.

Makin, T.R., Scholz, J., Henderson Slater, D., Johansen-Berg, H., Tracey, I., 2015. Reassessing cortical reorganization in the primary sensorimotor cortex following arm amputation. Brain 138, 2140–2146.

Miller, K.J., Abel, T.J., Hebb, A.O., Ojemann, J.G., 2011. Reorganization of large-scale physiology in hand motor cortex following hemispheric stroke. Neurology 76, 927–929.

Miller, K.J., Leuthardt, E.C., Schalk, G., Rao, R.P.N., Anderson, N.R., Moran, D.W., Miller, J.W., Ojemann, J.G., 2007. Spectral changes in cortical surface potentials during motor movement. J. Neurosci. 27, 2424–2432.

Miller, K.J., Schalk, G., Fetz, E.E., Den Nijs, M., Ojemann, J.G., Rao, R.P.N., 2010. Cortical activity during motor execution, motor imagery, and imagery-based online feedback. Proc. Natl. Acad. Sci. U. S. A. 107, 4430–4435.

Miller, K.J., Sorensen, L.B., Ojemann, J.G., Den Nijs, M., 2009a. Power-law scaling in the brain surface electric potential. PLoS Comput. Biol. 5, 1000609.

Miller, K.J., Zanos, S., Fetz, E.E., Den Nijs, M., Ojemann, J.G., 2009b. Decoupling the cortical power spectrum reveals real-time representation of individual finger movements in humans. J. Neurosci. 29, 3132–3137.

Moseley, G.L., 2006. Graded motor imagery for pathologic pain: a randomized controlled trial. Neurology 67, 2129–2134.

Nuttall, A.H., 1981. Some windows with very good sidelobe behavior. IEEE Trans. Acoust. 29, 84–91.

Papadelis, C., Kourtidou-Papadeli, C., Bamidis, P., Albani, M., 2007. Effects of imagery training on cognitive performance and use of physiological measures as an assessment tool of mental effort. Brain Cogn. 64, 74–85.

Penfield, W., Boldrey, E., 1937. Somatic motor and sensory representation in the cerebral cortex of man as studied by electrical stimulation. Brain 60, 389–443.

Proudfoot, M., Rohenkohl, G., Quinn, A., Colclough, G.L., Wuu, J., Talbot, K., Woolrich, M.W., Benatar, M., Nobre, A.C., Turner, M.R., 2017. Altered cortical beta-band oscillations reflect motor system degeneration in amyotrophic lateral sclerosis. Hum. Brain Mapp. 38, 237–254.

Qi, H.X., Stepniewska, I., Kaas, J.H., 2000. Reorganization of primary motor cortex in adult macaque monkeys with long-standing amputations. J. Neurophysiol. 84, 2133–2147.

Riva, N., Falini, A., Inuggi, A., Gonzalez-Rosa, J.J., Amadio, S., Cerri, F., Fazio, R., Del Carro, U., Comola, M., Comi, G., Leocani, L., 2012. Cortical activation to voluntary movement in amyotrophic lateral sclerosis is related to corticospinal damage: Electrophysiological evidence. Clin. Neurophysiol. 123, 1586–1592.

Röricht, S., Meyer, B.U., Niehaus, L., Brandt, S.A., 1999. Long-term reorganization of motor cortex outputs after arm amputation. Neurology 53, 106–111.

Roux, F.E., Lotterie, J.A., Cassol, E., Lazorthes, Y., Sol, J.C., Berry, I., Sindou, M.P., Schuele, S., Lüders, H., Burchiel, K.J., 2003. Cortical areas involved in virtual movement of phantom limbs: comparison with normal subjects. Neurosurgery 53, 1342–1353.

Salas, M.A., Bashford, L., Kellis, S., Jafari, M., Jo, H., Kramer, D., Shanfield, K., Pejsa, K., Lee, B., Liu, C.Y., Andersen, R.A., 2018. Proprioceptive and cutaneous sensations in humans elicited by intracortical microstimulation. Elife 7.

Schellekens, W., Petridou, N., Ramsey, N.F., 2018. Detailed somatotopy in primary motor and somatosensory cortex revealed by Gaussian population receptive fields. Neuroimage 179, 337–347.

Siero, J.C., Hermes, D., Hoogduin, H., Luijten, P.R., Petridou, N., Ramsey, N.F., 2013. BOLD consistently matches electrophysiology in human sensorimotor cortex at increasing movement rates: A combined 7T fMRI and ECoG study on neurovascular coupling. J. Cereb. Blood Flow Metab. 33, 1448–1456.

Siero, J.C.W., Hermes, D., Hoogduin, H., Luijten, P.R., Ramsey, N.F., Petridou, N., 2014. BOLD matches neuronal activity at the mm scale: a combined 7T fMRI and ECoG study in human sensorimotor cortex. Neuroimage 101, 177–184.

Smirnakis, S.M., Brewer, A.A., Schmid, M.C., Tolias, A.S., Schüz, A., Augath, M., Inhoffen, W., Wandell, B.A., Logothetis, N.K., 2005. Lack of long-term cortical reorganization after macaque retinal lesions. Nature 435, 300–307.

Talelli, P., Ewas, A., Waddingham, W., Rothwell, J.C., Ward, N.S., 2008a. Neural correlates of age-related changes in cortical neurophysiology. Neuroimage 40, 1772–1781.

Talelli, P., Waddingham, W., Ewas, A., Rothwell, J.C., Ward, N.S., 2008b. The effect of age on task-related modulation of interhemispheric balance. Exp. Brain Res. 186, 59–66.

Turner, J.A., Lee, J.S., Martinez, O., Medlin, A.L., Schandler, S.L., Cohen, M.J., 2001. Somatotopy of the motor cortex after long-term spinal cord injury or amputation. IEEE Trans. Neural Syst. Rehabil. Eng. 9, 154–160.

Valyear, K.F., Philip, B.A., Cirstea, C.M., Chen, P.W., Baune, N.A., Marchal, N., Frey, S.H., 2020. Interhemispheric transfer of post-amputation cortical plasticity within the human somatosensory cortex. Neuroimage 206.

van den Boom, M.A., Miller, K.J., Ramsey, N.F., Hermes, D., 2021. Functional MRI based simulations of ECoG grid configurations for optimal measurement of spatially distributed hand-gesture information. J. Neural Eng. 18.

Vansteensel, M.J., Pels, E.G.M., Bleichner, M.G., Branco, M.P., Denison, T., Freudenburg, Z.V., Gosselaar, P., Leinders, S., Ottens, T.H., Van Den Boom, M.A., Van Rijen, P.C., Aarnoutse, E.J., Ramsey, N.F., 2016. Fully implanted brain–computer interface in a locked-in patient with ALS. N. Engl. J. Med. 375, 2060–2066.

Verstynen, T., Diedrichsen, J., Albert, N., Aparicio, P., Ivry, R.B., 2005. Ipsilateral motor cortex activity during unimanual hand movements relates to task complexity. J. Neurophysiol. 93, 1209–1222.

Welch, P.D., 1967. The use of fast fourier transform for the estimation of power spectra: a method based on time averaging over short modified periodograms. IEEE Trans. Audio Electroacoust. 15, 70–73.

Wesselink, D.B., Van Den, H.F.M., Ejaz, N., Dempsey-Jones, H., Cardinali, L., Tarall-Jozwiak, A., Diedrichsen, J., Makin, T.R., 2019. Obtaining and maintaining cortical hand representation as evidenced from acquired and congenital handlessness. Elife 8.

Yanagisawa, T., Fukuma, R., Seymour, B., Hosomi, K., Kishima, H., Shimizu, T., Yokoi, H., Hirata, M., Yoshimine, T., Kamitani, Y., Saitoh, Y., 2016. Induced sensorimotor brain plasticity controls pain in phantom limb patients. Nat Commun. 7, 13209.

Yanagisawa, T., Fukuma, R., Seymour, B., Tanaka, M., Hosomi, K., Yamashita, O., Kishima, H., Kamitani, Y., Saitoh, Y., 2020. BCI training to move a virtual hand reduces phantom limb pain: a randomized crossover trial. Neurology 95, E417–E426.

Yanagisawa, T., Hirata, M., Saitoh, Y., Kishima, H., Matsushita, K., Goto, T., Fukuma, R., Yokoi, H., Kamitani, Y., Yoshimine, T., 2012. Electrocorticographic control of a prosthetic arm in paralyzed patients. Ann. Neurol. 71, 353–361.

Yang, T.T., Gallen, C., Schwartz, B., Bloom, F.E., Ramachandran, V.S., Cobb, S., 1994. Sensory maps in the human brain [13]. Nature.

Zanos, S., Miller, K.J., Ojemann, J.G., 2008. Electrocorticographic spectral changes associated with ipsilateral individual finger and whole hand movement. In: Proceedings of the 30th Annual International Conference of the IEEE Engineering in Medicine and Biology Society, EMBS'08 - "Personalized Healthcare through Technology.". IEEE Computer Society, pp. 5939–5942.